Electron spin echo envelope modulation spectroscopy in mixed alkali silicate glasses

Loukas Astrakas and George Kordas

Citation: The Journal of Chemical Physics **110**, 6871 (1999); doi: 10.1063/1.478592
View online: http://dx.doi.org/10.1063/1.478592
View Table of Contents: http://scitation.aip.org/content/aip/journal/jcp/110/14?ver=pdfcov
Published by the AIP Publishing

Electron spin echo envelope modulation spectroscopy in mixed alkali silicate glasses

Loukas Astrakas and George Kordas
Institute of Materials Science, National Center for Scientific Research Demokritos, 15310 Aghia Paraskevi Attikis, Greece

(Received 27 October 1998; accepted 13 January 1999)

Lithium and sodium silicate glasses of the x mole % Li_2O y mole % Na_2O (100-x-y) mole % SiO_2 composition with x, y between 10–50 were γ-irradiated at room temperature and subsequently studied by electron spin echo envelope modulation (ESEEM) spectroscopy at the X-band and 20 K temperature. Evaluation of the ESEEM spectra revealed weak magnetic coupling between the nonbridging oxygen (NBO) and the neighboring alkali metal. The covalent character between NBO and alkali metal is negligible, though it depends upon the kind weakly. The alkali metal occupies sites forming an angle of 60° with respect to the z-axis of the g-tensor. The magnetic couplings remain unchanged with the variation of the concentration of the alkali or the doping with another alkali. © *1999 American Institute of Physics.* [S0021-9606(99)51814-X]

I. INTRODUCTION

Alkali silicate glasses are of both industrial and scientific interest. One the one hand they form the basis of many commercial glasses. On the other hand the variation of their structure with the composition leads to alteration of their chemical and physical properties the explanation of which result in fundamental problems in glass as well as in earth sciences. One of the their most intriguing problems is the mixed-alkali effect, where the addition of a second alkali oxide results to orders of magnitude changes in their transport properties including diffusion and ionic conductivity.[1–3]

The structure of oxide glasses based on the Zachariasen–Warren model[4,5] can be described using SiO_4 - tetrahedra connected over the oxygen atoms (bridging oxygen BO) into a continuous random network (CRN) with distributions of the Si–O distances, Si–O–Si angles and dihedral angles. According to this model, the addition of alkali oxides interrupts the CRN through the formation of nonbridging oxygens (NBO).[6]

Many techniques have been used to elucidate the structure of silicate glasses including x-ray absorption fine structure (XAFS) spectroscopy,[7] magic angle spinning nuclear magnetic resonance (MASNMR),[8,9] neutron scattering,[10,11] lR,[12] Raman,[13] and x-ray photoemission spectroscopy (XPS).[14]

Despite the large amount of work, many questions are still open concerning the local cation environment or the spatial distribution of cations within the glass network. For example, there is no experimental evaluation of the nature of the NBO–Me (Me=Lin Na, and K) bond character. The bond strength is important for the understanding of the microscopic mechanism of ionic transport. When this is attempted from first principles,[15] the Andersson–Stuart approach is adopted,[16]

$$E_A=(\beta z z_o e^2)/(\gamma(r+r_o))+4\pi G r_D(r-r_D)^2, \qquad (1)$$

where, z_o and r_o are the charge and radius of the O^{2-} ion, respectively, β is the lattice parameter depending on the distance between neighboring sites, r is the cation radius, r_D is the radius of normal doorways in the glass, G is the elastic modulus, and γ is a covalence parameter.

This model has important shortcomings.[17] This approach assumes that the nature of the bond is electrostatic and the covalent character is introduced via a covalent factor γ. Then, γ is arbitrarily set equal to high frequency permittivity ϵ_∞. As it was perceived by Andersson and Stuart, it expresses ''the deformability of electron clouds on the oxygen atoms.'' The direct measurement of the bond character (covalent or ionic) in the NBO–Me bond is a crucial test of the Andersson–Stuart model.

Another important question closely related with percolation models[18,3] attempts to explain mixed alkali effect with the existence of ''favorable'' sites for each cation. EXAFS and molecular dynamics simulations[7,19] have suggested that each type of cation is located in rather distinct local sites in mixed alkali glasses, where MAS-NMR (Ref. 9) failed to give any evidence for like cation clustering.

In glasses, EPR can be applied to paramagnetic centers created through γ irradiation.[6,7] Whenever CW-EPR spectroscopy was applied to silicate glasses,[20,21] inhomogeneous broadening suppressed the resolution of weak couplings. The electron spin echo envelope modulation (ESEEM) spectroscopy[22,23] which is a pulsed EPR technique, can reveal these weak couplings[22–24] and thus offers a powerful tool for the detailed study of the microenvironment of the paramagnetic centers in solids. ESEEM arises when nonsecular electron–nuclear spin interactions are present and it is observed as a modulation of the echo intensity. In single-crystal samples, the modulation contains the nuclear-transition energies. In glasses, the random orientations of the hyperfine tensor relatively to the external magnetic field distribute the nuclear-transition energies and demand computer simulations for the proper analysis of the spectra. In complicated spectra a powerful method for the assignment of the

TABLE I. Molar composition of the samples.

No.	% Li	% Na
1	9.53	0
2	5.17	4.10
3	34.6	0
4	0	43.2
5	19.0	25.6

hyperfine couplings is the four-pulse two-dimensional hyperfine sublevel correlation spectroscopy (2D-HYSCORE).[25–29]

In the case of an electron spin interacting with a nuclear spin $I=3/2$, the ESEEM spectra are complicated.[30] ESEEM applications for $I=3/2$ (Refs. 31–33) as well as for glasses are fairly limited.[34–36] Recently, ESEEM was employed for $I=3/2$ case in glasses using borate and silicate compositions.[37–39]

In the present work, we report an ESEEM study of γ-irradiated alkali silicate glasses of the x mole % Li_2O y mole % Na_2O $(100\text{-}x\text{-}y)$ mole % SiO_2 composition with x, y between 10 and 50. We put emphasis on the anisotropic hyperfine interaction between alkali and NBO to determine the covalent character of oxygen-alkali bond. In contrast to the CW-EPR spectroscopy, the present ESEEM measurements can resolve the magnetic coupling between the electron spin and ^{6}L, ^{7}L, and ^{23}Na nuclei.

II. EXPERIMENT

A. Sample preparation

More than 15 alkali silicate glasses of the x mole % Li_2O y mole % Na_2O $(100\text{-}x\text{-}y)$ mole % SiO_2 composition with x, y between 0 and 50, prepared by the melting technique. Table I gives the composition of some representative glasses, whose spectra are presented in this paper. Batches of 30 g were put in alumina crucible at temperatures 300 °C above the melting point for 2 h, followed by splat cooling. The amorphous state was confirmed by XRD analysis using a D500 Siemens instrument. The stoichiometry was confirmed by ICP analysis using an Optima 3000 Perkin Elmer spectrometer. Finally, the samples were irradiated with a γ-^{60}Co source.

B. Spectroscopic measurements

Pulsed EPR experiments were performed at X-band with the Bruker ESP 380 spectrometer equipped with a dielectric resonator, an ITC4 Oxford low temperature control unit and an Oxford Instruments LQ-He-cryostat. The microwave frequency was measured with a HP 5350B microwave frequency counter. The instrument dead time was about 100 ns. In the three-pulse $(\pi/2\text{-}\tau\text{-}\pi/2\text{-}T\text{-}\pi/2)$ ESEEM data, the amplitude of the stimulated echo was measured as a function of $\tau+T$. The minimum interpulse T was 56 ns and was incremented in steps of 8 ns. The duration of the $\pi/2$ pulse was 16 ns. Measurements were carried out at 20 K with a repetition rate of 20 Hz and τ-values from 120 to 320 ns. 2D-HYSCORE spectra were recorded using the sequence $(\pi/2\text{-}\tau\text{-}\pi/2\text{-}t_1\text{-}\pi\text{-}t_2\text{-}\pi/2\text{-echo})$, where the echo is measured as a function of t_1 and t_2. The duration of the $\pi/2$ and π pulse was 16 ns and 32 ns with equal amplitudes, respectively. 256 points were recorded in each dimension for a series of τ values from 128 to 352 ns, while the t_1 and t_2 were incremented in steps of 16 ns from their initial value. Appropriate phase-cycling procedures in the stimulated-echo and HYSCORE experiments were applied in order to remove the unwanted echos.[41,42]

C. Data manipulation

1. 1D-stimulated echo ESEEM

Prior to Fourier transform, the time-domain echo decay was factored out by subtraction of a multiexponential function and zero filling to 1024 points was performed followed by a tapering with a Hamming window.

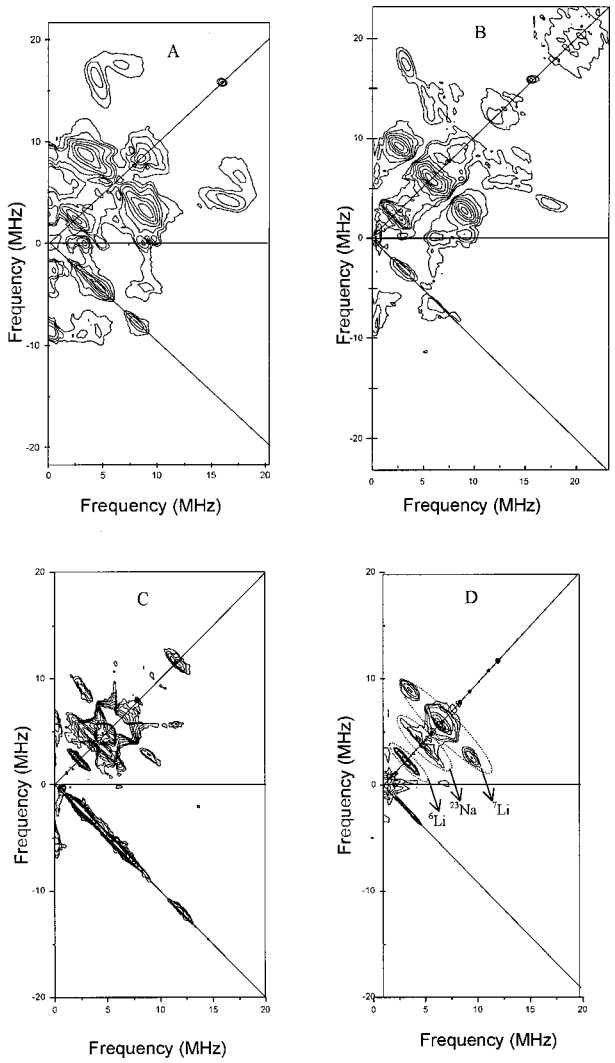

FIG. 1. Experimental 2D-HYSCORE spectrum (contour plots) of sample: (A) No. 1, (B) No. 3, (C) No. 5, and (D) No. 2 recorded at $\tau=128$ ns. The dashed areas in (D) indicate the contribution of each alkali nuclei in the spectrum. Experimental conditions, $t_1\times t_2=128\times128$ points; start values $t_1=56$ ns, $t_2=56$ ns, microwave frequency, 9.70 GHz; magnetic field strength 3455 G; sample temperature 20 K; time interval between successive pulse sets, 3 ms; 20 events were averaged; temperature=20 K.

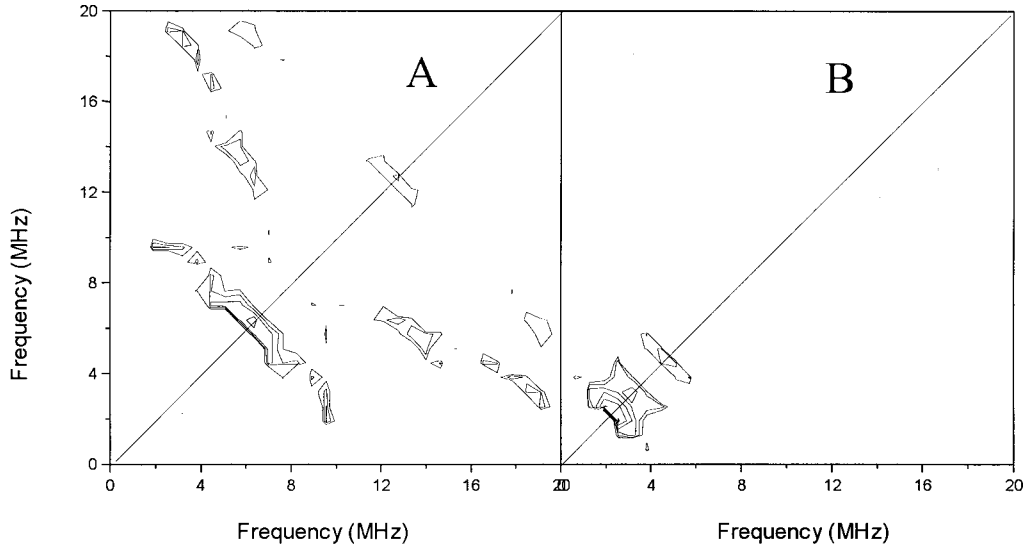

FIG. 2. Calculated HYSCORE (''stick'' spectrum without broadening) of (A) ^{7}Li and ^{6}Li nucleus and (B) Na nucleus for τ=128 ns with parameters given in Table II. ($t1\times t2=128\times128$ points.)

2. 2D-HYSCORE ESEEM

The background decay in both t_1 and t_2 dimensions was subtracted using a polynomial function followed by zero-filling to 512 points in two dimensions and tapering with a Hamming window; then Fourier transform was carried out in both dimensions.

III. RESULTS

A. ESEEM experiments

We have performed several 2D-HYSCORE experiments employing a series of different τ-intervals between the first two pulses in the four-pulse sequence, in order to eliminate the τ-suppression effect. Figures 1(A)–1(D) show representative contour plots of 2D-HYSCORE spectra recorded for τ=128 ns.

All HYSCORE spectra have the same symmetric ridges perpendicular to the diagonal at the alkali Larmor frequencies (2.16 MHz for ^{6}Li, 5.72 MHz for ^{7}Li, and 3.89 MHz for ^{23}Na. Also two cross-peaks (at 9 MHz, 2 MHz) are resolved in Figs. 1(B)–1(D). Finally, we notice cross peaks (at 3 MHz, 17 MHz and 5 MHz, 13 MHz) [Figs. 1(A) and 1(B)] and peaks on the diagonal at 12 MHz and 8 MHz [Figs. 1(B) and 1(C)]. Features parallel to the frequency axes [Figs. 1(A) and 1(B)] should be ignored because they are usually experimental artefacts due to inevitable imperfections of the π pulse, the phase cycling or the baseline correction. All the observed cross-peaks are located on the (+,+) quadrant.

B. Simulation of ESEEM spectra

The ESEEM three pulse-spectra contain the frequencies $\omega_{ij}^{\alpha,\beta}$ of the nuclear transition between the i and j nuclear sublevel within the same electron spin manifold, also known as ENDOR frequencies. These frequencies depend on the terms of the spin-Hamiltonian that describes the interaction of a $S=1/2$ center with one (or many) alkali nucleus with spin quantum number $I=3/2$. In our case the dominant terms are the hyperfine, the quadrupole and the Zeeman interactions. The two-dimensional HYSCORE spectra contain cross-peaks $(\omega_{ij}^{\alpha},\omega_{kl}^{\beta}),(\omega_{kl}^{\beta},\omega_{ij}^{\alpha})$ with coordinates ENDOR frequencies of different electron spin manifolds.

Figures 2(A) and 2(B) represent simulations of HYSCORE spectra (τ=128 ns) for ^{7}Li, ^{6}Li, and ^{23}Na, respectively. Table II gives the parameters of the simulations. For Li nuclei, the quadrupole interaction is negligible and was ignored in the calculations. For ^{23}Na, the adjustment of the asymmetry parameter η is uncertain because it had only second order effects on the spectral features.

Figures 3 and 4(B) are the experimental (solid line) and simulated (dotted line) spectra of three-pulse ESEEM for samples Nos. 1 and 4, respectively. In both simulations the contribution of the matrix nuclei has omitted. They contribute to the spectrum with a strong peak at the Larmore frequency of the corresponding alkali. The simulated spectra give only the contribution to the experimental spectra of the alkali nuclei near the paramagnetic center. It is clear that the matrix alkali nuclei account for the main part of the experimentally observed modulation and cover the contribution of the near alkali. In this case, HYSCORE is more suitable for the assignment of the various couplings and this can also be seen clearly from a direct comparison between Figs. 4(A) and 4(B).

IV. DISCUSSION

Reference 40 contains a detailed discussion for the HYSCORE spectra of sample No. 1 and their simulations. A

TABLE II. Alkali nuclear coupling parameters used for the calculation of ESEEM spectra.

	^{7}Li	^{6}Li	^{23}Na
e^2qQ/h(MHz)	$<$0.2	$\sim$0.0	1.0±0.4
T (MHz)	4±0.2	1.5±0.2	1.8±0.2
$A_{\rm ISO}$ (MHz)	0.5±0.1	0.2±0.05	1.0±0.1
β (deg)	60±20	60±20	60±20

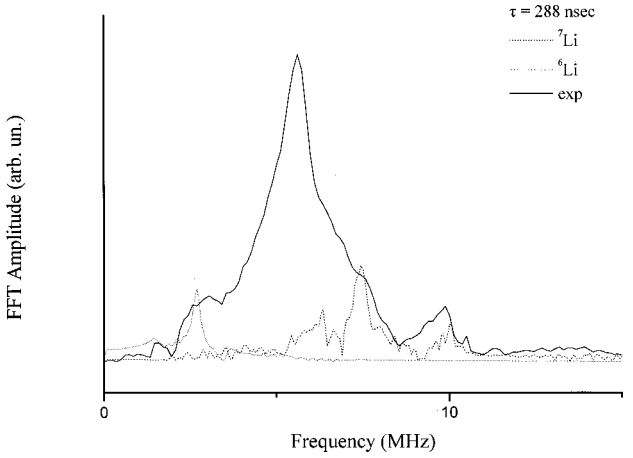

FIG. 3. Comparison between experimental three pulse ESEEM pattern (solid line) of sample No. 1 (τ=288 ns) and calculated Li modulation patterns (dotted lines) with parameters given in Table II.

new result here is that even without the simulations, a simple comparison of the HYSCORE spectra shows that for all samples the magnetic couplings of the alkali nuclei remain almost the same despite the concentration. Small differences are due to experimental reasons (imperfect π pulse, small deviations from resonance frequency, etc.). For an accurate evaluation of the ESEEM spectra, simulations were performed revealing the values T and A_{iso}. The anisotropic hfs interaction, T, according to the point-dipole gives the effective distance between the electron spin and the alkali nucleus, $r_{\mathrm{Me(=Li\ and\ Na)-NBO}}$. This distance was estimated for Li–NBO and Na–NBO to be equal to 2.0 ± 0.2 Å and 2.3 ± 0.2 Å, respectively. At low alkali concentrations, this represents the distance between the nonbridging oxygen and the alkali[20] and matches with the distance determined by the neutron diffraction and x-ray analysis of lithium silicate glasses.[7,43] Also, according to the point dipole approximation the z axis of the hyperfine tensor has the alkali-oxygen direction. Simple LCLO-MO calculations[17] showed that for low alkali concentrations the z principal axis of the g tensor has the Si–O direction. For high alkali concentrations, it has been suggested[17] that the spin lies between two neighbouring nonbridging oxygen so in this case the z principal axis of the g tensor connects the Si nucleus with the spin. Assuming that the same is valid in our case and using our result, that the angle between z axis of hyperfine and g tensor is always close to $60°\pm20°$, we present in Fig. 5 a working model consistent with the above, where the alkali cations occupy interstices of oxygen's polyhedra.[17] The fact that for all the samples the angle β is the same, it indicates the possibility that there are well-defined alkali equilibrium sites in the glass network, accessible for every cation.

Now, we would like to discuss the result concerning the A_{iso} values. A $2s$ orbital of ^{7}Li processes to an $A_{\mathrm{iso}}=364.9$ MHz.[44] We derived from the simulation $A_{\mathrm{iso}}=0.5$ MHz indicating a 0.13% ($=0.5/364.9$) contribution of this orbital to the unpaired electron spin density. Similarly, the measured $A_{\mathrm{iso}}=1$ MHz for ^{23}Na compared with the $A_{\mathrm{iSO}}=927.1$ MHz (Ref. 44) for a complete $3s$ orbital of ^{23}Na leads to an 0.11% contribution of the Na $3s$ orbital at the unpaired electron spin density. This means that the covalent character of alkali-oxygen bond is negligible and does not depend on the composition. Since the deformation of the oxygen's electron clouds does not affect the ionic character of the bond with the alkali, the dependence of alkali's binding energy on the concentration should be searched elsewhere, i.e., the existence of polarization terms seems to be more likely.[17] Other optical basicity measurements[45,46] have also tried to investigate the electronic state of the oxygen in mixed alkali glasses but in an indirect way, using as a probe Tl^{+}, and measuring large shifts in their UV spectra.[43] The advantage of the ESSEM technique is that it is highly selective and the ''probe'' ions are the alkali cations themselves.

V. CONCLUSION

ESEEM spectroscopy has been applied to γ-irradiated alkali silicate glasses. The 2D-HYSCORE experiment can

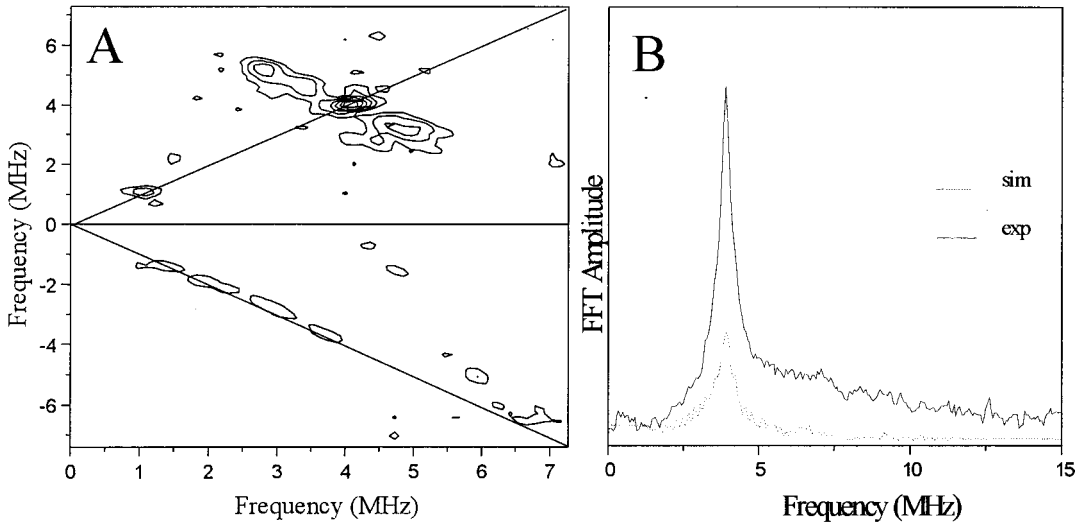

FIG. 4. (A) Experimental 2D-HYSCORE spectrum (contour plots) of sample No. 4. (B) Comparison between experimental three pulse ESEEM pattern (solid line) of sample No. 4 (τ=288 ns) and calculated Na modulation patterns (dotted line) with parameters given in Table II.

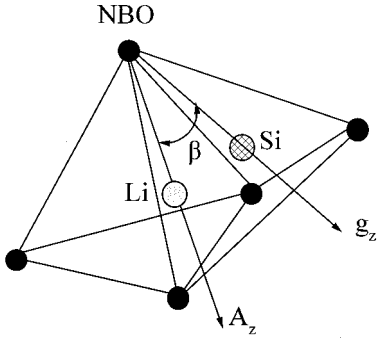

FIG. 5. Structural model for local environment of an alkali in alkali silicate glass. The alkali occupy oxygen's polyhedral interstices (tetrahedral in our example) interstices (Ref. 17). β is the angle between the z principal axes of the g (g_z) and the hyperfine (A_z) tensors. For the regular tetrahedral $\beta \cong 40°$.

unravel modulations, which are not well resolved in the three-pulse spectrum. The magnetic couplings between the paramagnetic centre and the alkali do not depend on the composition of the sample. The value of the anisotropic hyperfine interaction confirmed previous results[7,43] concerning the distance between the alkali and the nonbridging oxygen. Moreover, we show that the alkali occupy sites 60° away from the z principal axis of the g-tensor. The isotropic hyperfine interaction has small value despite the composition. This means that the Me(=Li,Na)–O bond is essentially ionic.

ACKNOWLEDGMENTS

We thank the Greek General Secretariat for Research and Technology and European Community for funding this research under Contract No. EIIET II 296. We also thank Dr. C. Trapalis for the ICP analysis and Dr. Y. Deligiannakis for his helpful discussions.

[1] O. Isard, J. Non-Cryst. Solids **1**, 235 (1996).
[2] D. E. Day, J. Non-Cryst. Solids **21**, 343 (1976).
[3] M. D. Ingram, Phys. Chem. Glasses **28**, 215 (1987).
[4] W. H. Zachariasen, J. Am. Chem. Soc. **54**, 3841 (1932).
[5] B. E. Warren, H. Krutter, and O. Morningstar, J. Am. Ceram. Soc. **19**, 202 (1936).
[6] B. E. Warren and J. Biscoe, J. Am. Ceram. Soc. **21**, 259 (1938).
[7] G. N. Greaves, J. Non-Cryst. Solids **71**, 203 (1985).
[8] I. Farnan, P. J. Grandinetti, J. H. Baltisberger, J. F. Stebbins, U. Werner, M. A. Eastman, and A. Pines, Nature (London) **358**, 21 (1992).
[9] B. Gee, M. Janssen and H. Eckert, J. Non-Cryst. Solids **215**, 41 (1997).
[10] P. H. Gaskell, in *The Physics of Noncrystalline Solids*, edited by L. D. Pye, W. C. LaCourse, and H. J. Stevens (Taylor and Francis, London, 1992), p. 15.
[11] A. G. Clare, A. C. Wright, and R. N. Sinclair, J. Non-Cryst. Solids **213/214**, 321 (1997).
[12] E. I. Kamitsos, A. P. Patsis, and G. D. Chryssikos, in *The Physics of Noncrystalline Solids*, edited by L. D. Pye, W. C. LaCourse, and H. J. Stevens (Taylor and Francis, London, 1992), p. 461.
[13] N. Umesaki, N. Iwamoto, M. Tatsumisago, and T. Minami, J. Non-Cryst. Solids **106**, 77 (1988).
[14] D. Sprenger, H. Bach, W. Meisel, and P. Gótlich, J. Non-Cryst. Solids **159**, 187 (1993).
[15] G. N. Greaves and K. L. Ngai, Phys. Rev. B **52**, 6358 (1995).
[16] O. L. Andersson and D. A. Stuart, J. Am. Ceram. Soc. **37**, 573 (1938).
[17] S. R. Elliot, J. Non-Cryst. Solids **160**, 29 (1993).
[18] A. Bunde, M. D. Ingram, and P Maass, J. Non-Cryst. Solids **31**, 241 (1978).
[19] C. Huang and A. N. Cormack, J. Chem. Phys. **95**, 3634 (1991).
[20] G. Kordas and H. J. Oel, Phys. Chem. Glasses **23**, 179 (1982); J. W. H. Shreuers, J. Chem. Phys. **47**, 818 (1967); D. L. Griscom, J. Non-Cryst. Solids **31**, 241 (1978).
[21] M. A. Karakassides, G. Kordas, E. Mylonas, and C. C. Trapalis, Mater. Sci. Eng., B **26**, 35 (1994).
[22] S. A. Dikanov and Y. D. Tsvetkov, *ESEEM Spectroscopy* (Chemical Rubber, Boca Raton, 1992).
[23] L. G. Rowan, E. L. Hahn, and W. B. Mims, Phys. Rev. A **138**, 4 (1965).
[24] L. Kevan, in *Time Domain Electron Spin Resonance*, edited by L. Kevan and R. N. Schwartz (Wiley, New York, 1979), p. 279.
[25] P. Høfer, A. Grupp, H. Nedenfóhr, and M. Mehring, Chem. Phys. Lett. **132**, 279 (1986); P. Høfer, J. Magn. Reson., Ser. A **111**, 77 (1994).
[26] J. J. Shane, P. Høfer, E. J. Reijerse, and E. J. De Boer, J. Magn. Reson. **99**, 596 (1992).
[27] S. A. Dikanov, R. I. Samoilova, J. A. Smieja, and M. K. Bowman, J. Am. Chem. Soc. **117**, 10579 (1995).
[28] V. Kofman, J. J. Shane, S. A. Dikanov, M. K. Bowman, J. Libman, A. Shanzer, and D. Goldfarb, J. Am. Chem. Soc. **117**, 12771 (1995).
[29] Y. Deligiannakis and A. W. Rutherford, J. Am. Chem. Soc. **119**, 4471 (1997).
[30] E. J. Reijerse and C. P. Keijzers, J. Magn. Reson. **71**, 83 (1987).
[31] J. Isoya, M. K. Bowman, J. R. Norris, and J. A. Weil, J. Chem. Phys. **78**, 1735 (1983); M. Narayana, L. Kevan, and S. Schlick, J. Phys. Chem. **86**, 196 (1982).
[32] S. H. Jang, H. I. Lee, J. McCracken, and J. E. Jackson, J. Am. Chem. Soc. **115**, 1263 (1993).
[33] R. Krimse, K. Kohler, U. Abram, R. Bottcher, L. Golic, and E. de Boer, Chem. Phys. **143**, 75 (1990).
[34] G. Kordas, Phys. Chem. Glasses **38**, 21 (1997).
[35] V. V. Kurshev, H. A. Buskmaster, and L. Tykarski, J. Chem. Phys. **101**, 10338 (1994).
[36] K. Arai, S. Yamasaki, J. Isoya, and H. Namikawa, J. Non-Cryst. Solids **196**, 216 (1996).
[37] Y. Deligiannakis, L. Astrakas, G. Kordas, and R. Smith, Phys. Rev. B **58**, 11420 (1998).
[38] G. Kordas, in Proceedings of the Second International Conference on Borate Glasse, Crystals, and Melts, edited by A. C. Wright, S. A. Feller, and A. C. Hannon, 1997, p. 148 (unpublished).
[39] G. Kordas, Phys. Chem. Glasses **39**, 21 (1996).
[40] L. Astrakas, Y. Deligiannakis, G. Mitrikas, and G. Kordas, J. Chem. Phys. **109**, 8612 (1998).
[41] J. M. Fauth, A. Schweiger, L. Braunschweiler, J. Forrer, and R. Ernst, J. Magn. Reson. **66**, 64 (1986).
[42] G. Gemperle, G. Aebli, A. Schweiger, and R. R. Ernst, J. Magn. Reson. **88**, 241 (1990).
[43] A. Dietzel, Z. Elektrochem. **48**, 9 (1942); A. C. Hannon, B. Vessal, and J. M. Parker, J. Non-Cryst. Solids **150**, 97 (1992).
[44] J. Morton and K. Preston, J. Magn. Reson. **30**, 577 (1977).
[45] J. A. Duffy and M. D. Ingram, J. Am. Chem. Soc. **93**, 6448 (1971).
[46] J. A. Duffy and M. D. Ingram, J. Non-Cryst. Solids **21**, 373 (1976); A. J. Bruce, J. A. Duffy, and M. D. Ingram, Phys. Chem. Glasses **22**, 104 (1981).